CARPATHIAN J. MATH.
Volume **40** (2024), No. 2,
Pages 535 - 557

Online version at https://www.carpathian.cunbm.utcluj.ro/
Print Edition: ISSN 1584 - 2851; Online Edition: ISSN 1843 - 4401
DOI: https://doi.org/10.37193/CJM.2024.02.19

A parallel inertial SP-iteration monotone hybrid algorithm for a finite family of G-nonexpansive mappings and its application in linear system, differential, and signal recovery problems

DAMRONGSAK YAMBANGWAI[1] and TANAKIT THIANWAN[2,*]

ABSTRACT. For solving a common fixed point of a finite family of G-nonexpansive mappings, we propose a parallel inertial SP-iteration monotone hybrid algorithm (PISPMHA). Weak convergence theorem is established for PISPMHA in Hilbert spaces endowed with graphs. Convergence behavior of PISPMHA is analyzed and discussed. As applications, we apply PISPMHA to solve linear system, differential, and signal recovery problems.

1. INTRODUCTION

Let $\mathcal{H}$ be a real Hilbert space with inner product $\langle .,. \rangle$ and the induced by norm $\|.\|$. Let $\mathcal{C}$ be a nonempty subset of $\mathcal{H}$. We identify the graph G with the pair $(V(G), E(G))$, where the set $V(G)$ of its vertices coincide with set $\mathcal{C}$ and the set of edges $E(G)$ contains $\Delta = \{(x, x) : x \in \mathcal{C}\}$, where the cartesian product $\mathcal{C} \times \mathcal{C}$'s diagonal is denoted by Δ. Additionally, no two edges of G are parallel. If a mapping $\mathcal{T} : \mathcal{C} \to \mathcal{C}$ preserves the edges of G (or if $\mathcal{T}$ is edge-preserving), it is said to be G-contraction, i.e.,

$$(x, y) \in E(G) \Rightarrow (\mathcal{T}x, \mathcal{T}y) \in E(G)$$

and the weights of G's edges are reduced in the following manner by $\mathcal{T}$: there exists $\alpha \in (0, 1)$ such that

$$(x, y) \in E(G) \Rightarrow \|\mathcal{T}x - \mathcal{T}y\| \leq \alpha\|x - y\|.$$

A mapping $\mathcal{T} : \mathcal{C} \to \mathcal{C}$ is said to be G-nonexpansive (see [3], Definition 2.3 (iii)) if $\mathcal{T}$ preserves edges of G, i.e.,

$$(x, y) \in E(G) \Rightarrow (\mathcal{T}x, \mathcal{T}y) \in E(G),$$

and T non-increases weights of edges of G in the following way:

$$(x, y) \in E(G) \Rightarrow \|\mathcal{T}x - \mathcal{T}y\| \leq \|x - y\|.$$

We denote the fixed point set of a mapping $\mathcal{T} : \mathcal{H} \to \mathcal{H}$ by $\mathcal{F}(\mathcal{T}) = \{x \in \mathcal{H} : \mathcal{T}x = x\}$.

In 1922, Banach [9] proved the existence of unique fixed point for contractions in a complete metric space. The most recent proof of the theorem used Banach spaces with a graph G, where $G = (V(G), E(G))$ is a directed graph with all loops included in the sets $V(G)$ of its vertices and $E(G)$ of its edges. By combination of the concepts in fixed point theory and graph theory, Banach G-contraction was introduced by Jachymaski [21] in complete metric space accompanied with the graph G where the set of vertex matches with the metric space, also see e.g. [7], [12], [13], [14], [24], [27], [29], [31].

Received: 20.10.2023. In revised form: 19.03.2024. Accepted: 25.03.2024
2020 *Mathematics Subject Classification.* 46T99, 47H09, 47H10, 47J25, 49M37, 54H25.
Key words and phrases. *parallel inertial SP-iteration, G-nonexpansive mapping, common fixed point, differential problem, signal recovery problem.*
Corresponding author: Tanakit Thianwan; tanakit.th@up.ac.th

In the last few decades investigations of fixed points by some iterative schemes for G-contraction, G-nonexpansive and G-monotone nonexpansive mappings have been studied extensively by various authors (see [1], [2], [3], [30], [32] and the references cited therein).

In 2017, Sridarat et al. [33] modified the SP-iteration process for three G-nonexpansive mappings $\mathcal{T}_1, \mathcal{T}_2$ and $\mathcal{T}_3$ as follows:

$$\begin{cases} z_n = (1-\gamma_n)x_n + \gamma_n \mathcal{T}_3 x_n, \\ y_n = (1-\beta_n)z_n + \beta_n \mathcal{T}_2 z_n, \\ x_{n+1} = (1-\alpha_n)y_n + \alpha_n \mathcal{T}_1 y_n, \ n \geq 0, \end{cases} \tag{1.1}$$

where $\{\alpha_n\}$, $\{\beta_n\}$ and $\{\gamma_n\}$ are appropriate real sequences in $[0, 1]$. They studied the weak and strong convergence of the iterative scheme (1.1) under proper conditions.

Glowinski and Le Tallec [18] used a three-step iterative strategy while studying elastoviscoplasticity, computing eigenvalues, and liquid crystal theory. It was shown in [18] that the three-step iterative procedure produces superior numerical results than the estimated iterations in two and one steps. In 1998, Haubruge, Nguyen, and Strodiot [20] investigated the convergence analysis of Glowinski and Le Tallec's three-step methods [18], and then used these methods to obtain new splitting-type algorithms for resolving variation inequalities, separable convex programming, and minimization of a sum of convex functions. Additionally, they demonstrated that under some circumstances, three-step iterations result in highly parallelized algorithms.

Other than that, many mathematicians have been interested in finding ways to accelerate the convergence of the algorithm. One such method is inertial extrapolation, which was first put out by Polyak [28] as an acceleration procedure. Several convex minimization issues based on the two-order in-time dynamical system's heavy ball approach were resolved using this methodology. Two iterative steps consist of inertial-type methods; the second step is derived from the preceding two iterations. These techniques are dedicated to being thought of as an effective strategy to deal with various iterative algorithms, particularly with the projection-based algorithms; for more information, refer to the works of [4], [8], [11], [25], [38], [39], [42].

Suantai et al. [36], also, e.g. [37], recently presented the convergence of the algorithm utilizing the shrinking projection technique with the parallel monotone hybrid method for approximating common fixed points of a finite family of G-nonexpansive mappings, employing the notion of Anh and Hieu [5], [6]. The algorithm's use has been made available for signal recovery in circumstances when the kind of noise present is unknown.

The scheme is defined as follows: $x_1 \in C, C_0 = C$,

$$\begin{cases} v_n^i = \alpha_n^i x_n + (1-\alpha_n^i)\mathcal{T}_i x_n, i = 1, 2, ..., N, \\ i_n = argmax\{\left\|v_n^i - x_n\right\| : i = 1, 2, ..., N\}, \overline{v}_n := v_n^{i_n}, \\ C_{n+1} = \{v \in C_n : \|v - \overline{v}_n\| \leq \|v - x_n\|\}, \\ x_{n+1} = P_{C_{n+1}} x_1, n \geq 1, \end{cases} \tag{1.2}$$

where $\{\alpha_n^i\} \subset [0, 1]$ and $\liminf_{n\to\infty} \alpha_n^i(1-\alpha_n^i) > 0$ for all i = 1, 2, ... , N. $\overline{v}_n$ is chosen by the optimization all v_n^i with x_n. After that, the closed convex set C_{n+1} was constructed by $\overline{v}_n$. Finally, the next approximation x_{n+1} is defined as the projection of x_1 on to C_{n+1}.

The main purpose of this paper is to construct a parallel inertial SP-iteration monotone hybrid algorithm for approximating common fixed points of a finite family of G-nonexpansive mappings in a Hilbert space endowed with a graph. This paper is organized as follows.

Sect. 2 provides the fundamental concepts and a few lemmas needed to prove our main result. Sect. 3 presents the main result. This part demonstrates the proposed method's weak convergence results under reasonable assumptions in a real Hilbert space endowed with a graph. Section 4 uses our suggested approach to deal with several issues involving linear systems, differential equations, and signal recovery.

2. Graph Basic Definitions

In this section, we review certain basic concepts about the connectedness of graphs. These notions can be found, for instance, in [22].

Suppose that x and y are vertices in a graph G. A path in G from x to y of length N ($N \in \mathbb{N} \cup \{0\}$) is a sequence $\{x_i\}_{i=0}^{N}$ of $N+1$ vertices such that $x_0 = x$, $x_N = y$ and $(x_i, x_{i+1}) \in E(G)$ for $i = 0, 1, \ldots N-1$. If a path connects any two vertices in a graph G, the graph is said to be connected. A directed graph $G = (V(G), E(G))$ is said to be transitive if, for any $x, y, z \in V(G)$ such that (x, y) and (y, z) are in $E(G)$, we have $(x, z) \in E(G)$. The set of edges $E(G)$ is said to be convex if $(x_i, y_i) \in E(G)$ for all $i = 1, 2, ..., N$ and $\alpha_i \in (0, 1)$ such that $\sum_{i=1}^{N} \alpha_i = 1$, then $(\sum_{i=1}^{N} \alpha_i x_i, \sum_{i=1}^{N} \alpha_i y_i) \in E(G)$. We denote G^{-1} the conversion of a graph G and

$$E(G^{-1}) = \{(x, y) \in \mathcal{X} \times \mathcal{X} : (y, x) \in E(G)\}.$$

Suppose that $x_0 \in V(G)$ and $\mathcal{A} \subseteq V(G)$. We say that $\mathcal{A}$ is dominated by x_0 if $(x_0, x) \in E(G)$ for all $x \in \mathcal{A}$. $\mathcal{A}$ dominates x_0 if for each $x \in \mathcal{A}$, $(x, x_0) \in E(G)$.

In this study, the weak convergence is shown by the symbol $\rightharpoonup$. The following lemmas are required in the inspection to support our main results.

Lemma 2.1 ([4]). *Let $\{\psi_n\}$, $\{\delta_n\}$ and $\{\alpha_n\}$ be the sequences in $[0, +\infty)$ such that $\psi_{n+1} \leq \psi_n + \alpha_n(\psi_n - \psi_{n-1}) + \delta_n$, for all $n \geq 1$, $\sum_{n=1}^{\infty} \delta_n < +\infty$ and there exists a real number a with $0 \leq \alpha_n \leq \alpha < 1$ for all $n \geq 1$. Then the followings hold:*
(i) $\sum_{n\geq 1}[\psi_n - \psi_{n-1}] < +\infty$ where $[t] = max\{t, 0\}$;
(ii) There exists $\psi^* \in [0, +\infty)$ such that $\lim_{n\to+\infty} \psi_n = \psi^*$.

Lemma 2.2 ([34]). *Let $\mathcal{X}$ be a Banach space satisfying Opial's condition and let $\{x_n\}$ be a sequence in $\mathcal{X}$. Let $u, v \in \mathcal{X}$ be such that $\lim_{n\to\infty} \|x_n - u\|$ and $\lim_{n\to\infty} \|x_n - v\|$ exist. If $\{x_{n_k}\}$ and $\{x_{m_k}\}$ are subsequences of $\{x_n\}$ which converge weakly to u and v, respectively, then $u = v$.*

Lemma 2.3 ([35]). *Let $\mathcal{C}$ be a nonempty, closed and convex subset of a Hilbert space $\mathcal{H}$ and $G = (V(G), E(G))$ a directed graph such that $V(G) = \mathcal{C}$. Let $\mathcal{T} : \mathcal{C} \to \mathcal{C}$ be a G-nonexpansive mapping and $\{u_n\}$ be a sequence in $\mathcal{C}$ such that $u_n \rightharpoonup u$ for some $u \in \mathcal{C}$. If there exists a subsequence $\{u_{n_k}\}$ of $\{u_n\}$ such that $(u_{n_k}, u) \in E(G)$ for all $k \in N$ and $\{u_n - \mathcal{T}u_n\} \to v$ for some $v \in \mathcal{H}$. Then $(I - \mathcal{T})u = v$.*

3. Main results

For a finite family of G-nonexpansive mappings in Hilbert spaces with a graph, we are now prepared to prove the weak convergence theorem for the parallel inertial SP-iteration monotone hybrid algorithm (PISPMHA) in this section.

Theorem 3.1. *Let $\mathcal{H}$ be a real Hilbert space and $G = (V(G), E(G))$ a transitive directed graph such that $E(G)$ is convex. Let $\mathcal{T}_i : \mathcal{H} \to \mathcal{H}$ be a family of G-nonexpansive mappings for all $i = 1, 2, ..., N$ such that $F = \cap_{i=1}^{N} F(\mathcal{T}_i) \neq \emptyset$. Suppose that $\{\theta_n\} \subset [0, \theta]$ for each $\theta \in (0, 1]$ and $\{\alpha_n^i\}$, $\{\beta_n^i\}$, $\{\gamma_n^i\} \subset [0, 1]$.*

Algorithm 1 : Parallel inertial SP-iteration monotone hybrid algorithm (PISPMHA)

initialization*: Take* $x_0, x_1 \in \mathcal{H}$. ***For*** $n \geq 1$*:*

Compute

$$\begin{aligned} w_n &= x_n + \theta_n(x_n - x_{n-1}), \\ z_n^i &= (1-\gamma_n^i)w_n + \gamma_n^i T_i w_n, \\ y_n^i &= (1-\beta_n^i)z_n^i + \beta_n^i T_i z_n^i, \\ h_n^i &= (1-\alpha_n^i)y_n^i + \alpha_n^i T_i y_n^i, \\ x_{n+1} &= argmax\{\|h_n^i - w_n\|, i = 1, 2, ..., N\}. \end{aligned}$$

Let $\{x_n\}$ *and* $\{w_n\}$ *be the sequences generated by Algorithm 1 such that the following additional conditions hold:*
(i) $\sum_{n=1}^{\infty} \theta_n \|x_n - x_{n-1}\| < \infty$ *;*
(ii) $\{w_n\}$ *is dominated by t and* $\{w_n\}$ *dominates t for all* $t \in F$*, and if there exists a subsequence* $\{w_{n_k}\}$ *of* $\{w_n\}$ *such that* $\{w_{n_k}\} \rightharpoonup u \in \mathcal{H}$*, then* $(\{w_{n_k}\}, u) \in E(G)$*;*
(iii) $0 < \liminf_{n\to\infty} \gamma_n^i \leq \limsup_{n\to\infty} \gamma_n^i < 1$.
Then the sequence $\{x_n\}$ *converges weakly to an element in F.*

Proof. Let $t \in F$. Since $\{w_n\}$ dominates t and $\mathcal{T}_i$ is edge-preserving, we get $(\mathcal{T}_i w_n, t) \in E(G)$ for all $i = 1, 2, ..., N$. Implying there by $(z_n^i, t) = ((1-\gamma_n^i)w_n + \gamma_n^i \mathcal{T}_i w_n, t) \in E(G)$ by $E(G)$ is convex. Again, by edge-preserving of $\mathcal{T}_i (i = 1, 2, ..., N)$ and $(z_n^i, t) \in E(G)$, we have $(\mathcal{T}_i z_n^i, t) \in E(G)$, then $(y_n^i, t) = ((1-\beta_n^i)z_n^i + \beta_n^i \mathcal{T}_i z_n^i, t) \in E(G)$, since $E(G)$ is convex. For all $i = 1, 2, ..., N$, we get

$$\begin{aligned} \|h_n^i - t\| &= \left\|(1-\alpha_n^i)(y_n^i - t) + \alpha_n^i(\mathcal{T}_i y_n^i - t)\right\| \\ &\leq (1-\alpha_n^i)\left\|y_n^i - t\right\| + \alpha_n^i\left\|\mathcal{T}_i y_n^i - t\right\| \\ &\leq (1-\alpha_n^i)\left\|y_n^i - t\right\| + \alpha_n^i\left\|y_n^i - t\right\| \\ &= \left\|y_n^i - t\right\| \\ &= \left\|(1-\beta_n^i)(z_n^i - t) + \beta_n^i(\mathcal{T}_i z_n^i - t)\right\| \\ &\leq (1-\beta_n^i)\left\|z_n^i - t\right\| + \beta_n^i\left\|\mathcal{T}_i z_n^i - t\right\| \\ &\leq (1-\beta_n^i)\left\|z_n^i - t\right\| + \beta_n^i\left\|z_n^i - t\right\| \\ &= \left\|z_n^i - t\right\| \\ &= \left\|(1-\gamma_n^i)(w_n - t) + \gamma_n^i(\mathcal{T}_i w_n - t)\right\| \\ &\leq (1-\gamma_n^i)\|w_n - t\| + \gamma_n^i\|\mathcal{T}_i w_n - t\| \\ &\leq (1-\gamma_n^i)\|w_n - t\| + \gamma_n^i\|w_n - t\| \\ &= \|w_n - t\| \\ &\leq \|x_n - t\| + \theta_n\|x_n - x_{n-1}\|. \end{aligned}$$

This implies that $\|x_{n+1} - t\| \leq \|x_n - t\| + \theta_n\|x_n - x_{n-1}\|$. From Lemma 2.1 and the assumption (i), we obtain $\lim_{n\to\infty}\|x_n - t\|$ exists, in particular, $\{x_n\}$ is bounded and also

$\{z_n^i\}$, $\{y_n^i\}$ and $\{h_n^i\}$. By the properties in a real Hilbert space $\mathcal{H}$, we have

$$\begin{aligned}
\left\|h_n^i - t\right\|^2 &= \left\|((1-\alpha_n^i)y_n^i + \alpha_n^i \mathcal{T}_i y_n^i) - t\right\|^2 \\
&\leq (1-\alpha_n^i)\left\|y_n^i - t\right\|^2 + \alpha_n^i \left\|\mathcal{T}_i y_n^i - t\right\|^2 - (1-\alpha_n^i)\alpha_n^i \left\|y_n^i - \mathcal{T}_i y_n^i\right\|^2 \\
&\leq (1-\alpha_n^i)\left\|y_n^i - t\right\|^2 + \alpha_n^i \left\|\mathcal{T}_i y_n^i - t\right\|^2 \\
&\leq (1-\alpha_n^i)\left\|y_n^i - t\right\|^2 + \alpha_n^i \left\|y_n^i - t\right\|^2 \\
&= \left\|y_n^i - t\right\|^2 \\
&= \left\|((1-\beta_n^i)z_n^i + \beta_n^i \mathcal{T}_i z_n^i) - t\right\|^2 \\
&\leq (1-\beta_n^i)\left\|z_n^i - t\right\|^2 + \beta_n^i \left\|\mathcal{T}_i z_n^i - t\right\|^2 - (1-\beta_n^i)\beta_n^i \left\|z_n^i - \mathcal{T}_i z_n^i\right\|^2 \\
&\leq (1-\beta_n^i)\left\|z_n^i - t\right\|^2 + \beta_n^i \left\|\mathcal{T}_i z_n^i - t\right\|^2 \\
&\leq (1-\beta_n^i)\left\|z_n^i - t\right\|^2 + \beta_n^i \left\|z_n^i - t\right\|^2 \\
&= \left\|z_n^i - t\right\|^2 \\
&= \left\|((1-\gamma_n^i)w_n + \gamma_n^i \mathcal{T}_i w_n) - t\right\|^2 \\
&\leq (1-\gamma_n^i)\left\|w_n - t\right\|^2 + \gamma_n^i \left\|\mathcal{T}_i w_n - t\right\|^2 - (1-\gamma_n^i)\gamma_n^i \left\|w_n - \mathcal{T}_i w_n\right\|^2 \\
&\leq (1-\gamma_n^i)\left\|w_n - t\right\|^2 + \gamma_n^i \left\|w_n - t\right\|^2 - (1-\gamma_n^i)\gamma_n^i \left\|w_n - \mathcal{T}_i w_n\right\|^2 \\
&= \left\|w_n - t\right\|^2 - (1-\gamma_n^i)\gamma_n^i \left\|\mathcal{T}_i w_n - w_n\right\|^2 \\
&\leq \left\|x_n - t\right\|^2 + 2\theta_n \left\langle x_n - x_{n-1}, w_n - t\right\rangle - (1-\gamma_n^i)\gamma_n^i \left\|\mathcal{T}_i w_n - w_n\right\|^2. \qquad (3.3)
\end{aligned}$$

This implies that there exist $i_n \in \{1, 2, ..., N\}$ such that

$$(1-\gamma_n^{i_n})\gamma_n^{i_n} \left\|\mathcal{T}_{i_n} w_n - w_n\right\|^2 \leq \left\|x_n - t\right\|^2 - \left\|x_{n+1} - t\right\|^2 + 2\theta_n \left\langle x_n - x_{n-1}, w_n - t\right\rangle. \qquad (3.4)$$

By the assumption (i) and (iii), from (3.3), (3.4) and $\lim_{n\to\infty}\left\|x_n - t\right\|$ exist, we have

$$\lim_{n\to\infty} \left\|\mathcal{T}_{i_n} w_n - w_n\right\| = 0. \qquad (3.5)$$

In addition,

$$\left\|z_n^{i_n} - w_n\right\| \leq \gamma_n^{i_n} \left\|\mathcal{T}_{i_n} w_n - w_n\right\|. \qquad (3.6)$$

Using (3.5) and (3.6), we have

$$\lim_{n\to\infty} \left\|z_n^{i_n} - w_n\right\| = 0. \qquad (3.7)$$

Using (3.5), we also have

$$\begin{aligned}
\left\|z_n^{i_n} - \mathcal{T}_{i_n} w_n\right\| &\leq (1-\gamma_n^{i_n})\left\|w_n - \mathcal{T}_{i_n} w_n\right\| + \gamma_n^{i_n} \left\|\mathcal{T}_{i_n} w_n - \mathcal{T}_{i_n} w_n\right\| \\
&= (1-\gamma_n^{i_n})\left\|w_n - \mathcal{T}_{i_n} w_n\right\| \\
&\to 0 \ (as\ n \to \infty). \qquad (3.8)
\end{aligned}$$

Since (w_n, t), $(t, z_n^{i_n}) \in E(G)$, so $(w_n, z_n^{i_n}) \in E(G)$. From (3.7) and (3.8), we have

$$\begin{aligned}
\left\|y_n^{i_n} - \mathcal{T}_{i_n} w_n\right\| &\leq (1-\beta_n^{i_n})\left\|z_n^{i_n} - \mathcal{T}_{i_n} w_n\right\| + \beta_n^{i_n} \left\|\mathcal{T}_{i_n} z_n^{i_n} - \mathcal{T}_{i_n} w_n\right\| \\
&\leq (1-\beta_n^{i_n})\left\|z_n^{i_n} - \mathcal{T}_{i_n} w_n\right\| + \beta_n^{i_n} \left\|z_n^{i_n} - w_n\right\| \\
&\to 0 \ (as\ n \to \infty). \qquad (3.9)
\end{aligned}$$

Using (3.5) and (3.9), we have

$$\begin{aligned}\left\|y_n^{i_n}-w_n\right\| &= \left\|y_n^{i_n}-\mathcal{T}_{i_n}w_n+\mathcal{T}_{i_n}w_n-w_n\right\| \\ &\leq \left\|y_n^{i_n}-\mathcal{T}_{i_n}w_n\right\|+\left\|\mathcal{T}_{i_n}w_n-w_n\right\| \\ &\to 0 \ (as\ n\to\infty). \end{aligned} \tag{3.10}$$

Since (w_n,t), $(t,y_n^{i_n})\in E(G)$, so $(w_n,y_n^{i_n})\in E(G)$. It follows from (3.9) and (3.10) that

$$\begin{aligned}\left\|x_{n+1}-\mathcal{T}_{i_n}w_n\right\| &\leq (1-\alpha_n^{i_n})\left\|y_n^{i_n}-\mathcal{T}_{i_n}w_n\right\|+\alpha_n^{i_n}\left\|\mathcal{T}_{i_n}y_n^{i_n}-\mathcal{T}_{i_n}w_n\right\| \\ &\leq (1-\alpha_n^{i_n})\left\|y_n^{i_n}-\mathcal{T}_{i_n}w_n\right\|+\alpha_n^{i_n}\left\|y_n^{i_n}-w_n\right\| \\ &\to 0 \ (as\ n\to\infty). \end{aligned} \tag{3.11}$$

In addtion,

$$\left\|x_{n+1}-w_n\right\| \leq \left\|x_{n+1}-\mathcal{T}_{i_n}w_n\right\|+\left\|\mathcal{T}_{i_n}w_n-w_n\right\|.$$

From (3.5) and (3.11), we have

$$\lim_{n\to\infty}\left\|x_{n+1}-w_n\right\|=0. \tag{3.12}$$

It follows from (3.12) that

$$\left\|h_n^i-w_n\right\| \leq \left\|x_{n+1}-w_n\right\|\to 0 \tag{3.13}$$

as $n\to\infty$ for all $i=1,2,...,N$. From (3.3), we have

$$(1-\gamma_n^i)\gamma_n^i\left\|\mathcal{T}_iw_n-w_n\right\|^2 \leq \left\|w_n-t\right\|^2-\left\|h_n^i-t\right\|^2. \tag{3.14}$$

By our assumption (iii), it follows from (3.13) and (3.14) that

$$\lim_{n\to\infty}\left\|\mathcal{T}_iw_n-w_n\right\|=0 \tag{3.15}$$

for all $i=1,2,...,N$. Since $\{w_n\}$ is bounded and $\mathcal{H}$ is reflexive, $\omega_w(w_n)=\{x\in\mathcal{H}: w_{n_k}\rightharpoonup p, \{w_{n_k}\}\subset\{w_n\}\}$ is nonempty. Let $p\in\omega_w(w_n)$ be an arbitrary element. Then there exists a subsequence $\{w_{n_k}\}\subset\{w_n\}$ converging weakly to p. Let $q\in\omega_w(w_n)$ and $\{w_{n_m}\}\subset\{w_n\}$ be such that $w_{n_m}\rightharpoonup q$. Using Lemma 2.3 and (3.15), we have $p,q\in F$. Applying Lemma 2.2, we obtain $p=q$. The proof is completed. □

Note that if $\mathcal{T}$ is nonexpansive, then $\mathcal{T}$ is G-nonexpansive. As a direct convergence of Theorem 3.1, we can get the following result.

Corollary 3.1. *Let $\mathcal{H}$ be a real Hilbert space and $\mathcal{T}_i:\mathcal{H}\to\mathcal{H}$ a family of nonexpansive mappings for all $i=1,2,...,N$ such that $F=\cap_{i=1}^N F(\mathcal{T}_i)\neq\emptyset$. Let $\{x_n\},\{w_n\}$ generated by $x_0,x_1\in\mathcal{H}$ and*

$$\begin{cases} w_n = x_n+\theta_n(x_n-x_{n-1}), \\ z_n^i = (1-\gamma_n^i)w_n+\gamma_n^i\mathcal{T}_iw_n, \\ y_n^i = (1-\beta_n^i)z_n^i+\beta_n^i\mathcal{T}_iz_n^i, \\ h_n^i = (1-\alpha_n^i)y_n^i+\alpha_n^i\mathcal{T}_iy_n^i, \\ x_{n+1} = argmax\{\|h_n^i-w_n\|, i=1,2,...,N\}, \end{cases} \tag{3.16}$$

where $\{\theta_n\}\subset[0,\theta]$ for each $\theta\in(0,1]$ and $\{\alpha_n^i\}$, $\{\beta_n^i\}$, $\{\gamma_n^i\}\subset[0,1]$. Assume that the following additional conditions hold:
(i) $\sum_{n=1}^{\infty}\theta_n\left\|x_n-x_{n-1}\right\|<\infty$;
(ii) $0<\liminf_{n\to\infty}\gamma_n^i\leq\limsup_{n\to\infty}\gamma_n^i<1$.
Then the sequence $\{x_n\}$ converges weakly to an element in F.

4. APPLICATIONS

In this section, we apply the PISPMHA to solve certain linear system problems, differential problems, and signal recovery under situations without knowing the type of noises.

4.1. **Linear System problems.** Let consider the linear system

$$A\mathbf{x} = \mathbf{b}, \tag{4.17}$$

where $A : \mathbb{R}^l \to \mathbb{R}^l$ is linear and positive operator and $\mathbf{x}, \mathbf{b} \in \mathbb{R}^l$. Then, linear system (4.17) has a unique solution. There are many different ways of rearranging equation (4.17) in the form of fixed point equation $\mathcal{T}(x) = x$. For example, also see e.g. Table 1, the well-known weight Jacobi (WJ) and successive over relaxation (SOR) methods (see for example [19, 40, 41]) present the linear system (4.17) into the form of fixed point equation as

$$\mathcal{T}_{\text{WJ}}(\mathbf{x}) = \mathbf{x}, \quad \mathcal{T}_{\text{SOR}}(\mathbf{x}) = \mathbf{x} \quad \text{and} \quad \mathcal{T}_{\text{GS}}(\mathbf{x}) = \mathbf{x},$$

respectively.

Linear system	Fixed point mapping $T(\mathbf{x})$
$A\mathbf{x} = \mathbf{b}$	$\mathcal{T}_{\text{WJ}}(\mathbf{x}) = \left(I - \omega D^{-1}A\right)\mathbf{x} + \omega D^{-1}\mathbf{b}$
	$\mathcal{T}_{\text{SOR}}(\mathbf{x}) = \left(I - \omega\left(D - \omega L\right)^{-1}A\right)\mathbf{x} + \omega\left(D - \omega L\right)^{-1}\mathbf{b}$

TABLE 1. The different way of rearranging linear systems (4.17) into the form $x = \mathcal{T}(x)$.

And ω is weight parameter, D is the diagonal part of matrix A and L is the lower triangular part of matrix $D - A$, respectively.

In controlling the operators $\mathcal{T}_{\text{WJ}}$ and $\mathcal{T}_{\text{SOR}}$ in the form of $\mathcal{T}_{\text{WJ}}(\mathbf{h}) = \mathcal{S}_{\text{WJ}}(\mathbf{h}) + \mathcal{C}_{\text{WJ}}$, where

$$\mathcal{S}_{\text{WJ}} = I - \omega D^{-1}A, \quad \mathcal{C}_{\text{WJ}} = \omega D^{-1}\mathbf{G}$$

and $\mathcal{T}_{\text{SOR}}\mathbf{h} = \mathcal{S}_{\text{SOR}}\mathbf{h} + \mathcal{C}_{\text{SOR}}$, where

$$\mathcal{S}_{\text{SOR}} = I - \omega\left(D - \omega L\right)^{-1}A, \quad \mathcal{C}_{\text{SOR}} = \omega\left(D - \omega L\right)^{-1}\mathbf{G}$$

be nonexpansive mapping, see [17] for more detail, their weight parameter must be properly modified. The implemented of weight parameter ω for the operator $\mathcal{S}$ of WJ and SOR methods are defined as its norm less than one. Moreover, the optimal weight parameter ω_o in getting the smallest norm for each types of operator $\mathcal{S}$ are indicated on Table 2.

The different types of operator $\mathcal{S}$	Implement weight parameter ω	Optimal weight parameter ω_o
$\mathcal{S}_{\text{WJ}}$	$0 < \omega < \dfrac{2}{\lambda_{\max}(D^{-1}A)}$	$\omega_o = \dfrac{2}{\lambda_{\min}(D^{-1}A) + \lambda_{\max}(D^{-1}A)}$
$\mathcal{S}_{\text{SOR}}$	$0 < \omega < 2$	$\omega_o = \dfrac{2}{1 + \sqrt{1 - \rho^2}}$

TABLE 2. Implemented weight parameter and optimal weight parameter of operator $\mathcal{S}$.

The parameters $\lambda_{\max}(D^{-1}A)$ and $\lambda_{\min}(D^{-1}A)$ are the maximum and minimum eigenvalue of matrix $D^{-1}A$, respectively. ρ is the spectral radius of the iteration matrix of the Jacobi method ($\mathcal{S}_{\text{WJ}}$ with $\omega = 1$).

Thus, in finding the solution of linear system (4.17), we can manipulate this linear system into the form of fixed point equations

$$\mathcal{T}_i(\mathbf{x}) = \mathbf{x}, \quad \forall i = 1, 2, \ldots, M, \tag{4.18}$$

where $\mathbf{x}$ is the common solution of equation (4.18). We introduce a PISPMHA in solving the common solution of equation (4.18). The generated sequence $\{\mathbf{x}_n\}$ is created iteratively by using two initial data $\mathbf{x}_0, \mathbf{x}_1 \in \mathbb{R}^l$ and

$$\begin{aligned}
\mathbf{w}_n &= \mathbf{x}_n + \theta_n(\mathbf{x}_n - \mathbf{x}_{n-1}),\\
\mathbf{z}_n^i &= (1-\gamma_n^i)\mathbf{w}_n + \gamma_n^i \mathcal{T}_i(\mathbf{w}_n),\\
\mathbf{y}_n^i &= (1-\beta_n^i)\mathbf{z}_n^i + \beta_n^i \mathcal{T}_i(\mathbf{z}_n^i),\\
\mathbf{h}_n^i &= (1-\alpha_n^i)\mathbf{y}_n^i + \alpha_n^i \mathcal{T}_i(\mathbf{y}_n^i),\\
\mathbf{x}_{n+1} &= \text{argmax}\left\{||\mathbf{h}_n^i - \mathbf{w}_n||, i = 1, 2, \ldots, M\right\},
\end{aligned} \tag{4.19}$$

where $n \geq 1$ and $\{\alpha_n^i\}, \{\beta_n^i\}, \{\gamma_n^i\}$ are appropriate real sequences in $[0, 1]$. The following stopping criterion is used

$$\|\mathbf{x}_{n+1} - \mathbf{x}_n\|_2 < \epsilon_l,$$

and after that set $\mathbf{x}_{n-1} = \mathbf{x}_n$ and $\mathbf{x}_n = \mathbf{x}_{n+1}$.

Next, the PISPMHA (4.19) is compared with the well known WJ, SOR and Gauss-Seidel (the SOR with $\omega = 1$ names as GS) methods in getting the solution of linear system:

$$\begin{bmatrix}
4 & -1 & 0 & -1 & 0 & \ldots & \ldots & \ldots & 0\\
-1 & 4 & -1 & 0 & -1 & 0 & \ldots & \ldots & 0\\
0 & -1 & 4 & -1 & 0 & -1 & 0 & \ldots & 0\\
-1 & 0 & -1 & 4 & -1 & 0 & -1 & \ldots & 0\\
\vdots & \ddots & \ddots & \ddots & \ddots & \ddots & \ddots & \ddots & \vdots\\
0 & \ldots & -1 & 0 & -1 & 4 & -1 & 0 & -1\\
0 & \ldots & 0 & -1 & 0 & -1 & 4 & -1 & 0\\
0 & \ldots & \ldots & 0 & -1 & 0 & -1 & 4 & -1\\
0 & \ldots & \ldots & \ldots & 0 & -1 & 0 & -1 & 4
\end{bmatrix}_{l\times l}
\begin{bmatrix} x_1\\ x_2\\ x_3\\ x_4\\ \vdots\\ x_{l-3}\\ x_{l-2}\\ x_{l-1}\\ x_l \end{bmatrix}_{l\times 1}
= \begin{bmatrix} 1\\ 1\\ 1\\ 1\\ \vdots\\ 1\\ 1\\ 1\\ 1 \end{bmatrix}_{l\times 1}, \tag{4.20}$$

and $x_0 = [1 \quad 1 \quad \cdots \quad 1 \quad 1]^{\mathcal{T}}_{l\times 1}$, $x_1 = [0.5 \quad 0.5 \quad \cdots \quad 0.5 \quad 0.5]^{\mathcal{T}}_{l\times 1}$ with $l = 50, 100, 150$. For simplicity, the PISPMHA (4.19) with $M \leq 3$ and the G-nonexpansive mapping $\mathcal{T}_i$ are chosen from $\mathcal{T}_{\text{WJ}}, \mathcal{T}_{\text{SOR}}$ and $\mathcal{T}_{\text{GS}}$. The results of WJ, GS, SOR and the PISPMHA with the following cases:

Case I: The PISPMHA with $\mathcal{T}_{\text{WJ}}$
Case II: The PISPMHA with $\mathcal{T}_{\text{GS}}$
Case III: The PISPMHA with $\mathcal{T}_{\text{SOR}}$
Case IV: The PISPMHA with $\mathcal{T}_{\text{WJ}}$–$\mathcal{T}_{\text{GS}}$
Case V: The PISPMHA with $\mathcal{T}_{\text{WJ}}$–$\mathcal{T}_{\text{SOR}}$
Case VI: The PISPMHA with $\mathcal{T}_{\text{GS}}$–$\mathcal{T}_{\text{SOR}}$
Case VII: The PISPMHA with $\mathcal{T}_{\text{WJ}}$– $\mathcal{T}_{\text{GS}}$–$\mathcal{T}_{\text{SOR}}$

in solving linear system (4.20) are demonstrated and discussed. The weight parameter ω of the PISPMHA set as its optimum weight parameter (ω_o) defined on Table 2. We used the following parameters:

$$\alpha_n^i = \frac{n}{n+1}, \quad \beta_n^i = \alpha_n^i, \quad \gamma_n^i = \alpha_n^i, \tag{4.21}$$

$$\theta_n = \begin{cases} \min\left\{\dfrac{1}{n^2\|\mathbf{x}_n - \mathbf{x}_{n-1}\|_2^2}, 0.1\right\} & \text{if } (\mathbf{x}_n \neq \mathbf{x}_{n-1}) \;\&\; (1 \leq n < \widetilde{N}),\\ 0.15 & \text{otherwise,} \end{cases} \tag{4.22}$$

when $\widetilde{N}$ is a number of iterations that we want to stop with $\epsilon_l = 10^{-7}$. The approximate error per step of iteration for WJ, GS, SOR and all cases studies of the PISPMHA are measured by using the relative error

$$\|\mathbf{x_n} - \mathbf{x}\|_2 / \|\mathbf{x}\|_2.$$

Figures 1 and 2 show the relative error on each step of iteration and the iterations number throughout the process for WJ, GS, SOR and all cases studies of the PISPMHA in solving linear system (4.20) with $l = 50$, $l = 100$ and $l = 150$, respectively.

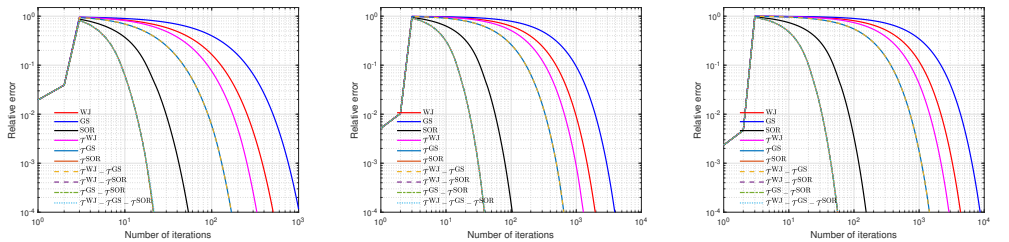

FIGURE 1. Relative error of the suggested methods to problem (4.20) with $l = 50$, $l = 100$ and $l = 150$, respectively.

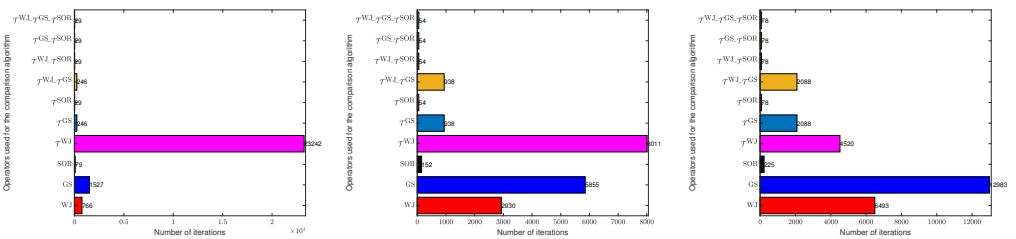

FIGURE 2. The evolution of iterations number for the suggested approach to problem (4.17) with $l = 50$, $l = 100$ and $l = 150$, respectively.

It can be seen from Figures 1 and 2 that when the relative error per each step of iteration and the iterations number throughout the process are compared, the SOR method is better than WJ, GS, $\mathcal{T}_{\text{WJ}}$, $\mathcal{T}_{\text{GS}}$ and $\mathcal{T}_{\text{WJ}}$–$\mathcal{T}_{\text{GS}}$ methods. And, the proposed approach with $\mathcal{T}_{\text{SOR}}$, $\mathcal{T}_{\text{WJ}}$–$\mathcal{T}_{\text{SOR}}$, $\mathcal{T}_{\text{GS}}$–$\mathcal{T}_{\text{SOR}}$ and $\mathcal{T}_{\text{WJ}}$–$\mathcal{T}_{\text{GS}}$–$\mathcal{T}_{\text{SOR}}$ are the same and better than SOR method. Moreover, the relative error per each step of iteration for the proposed approach and the iterations number throughout the process with $M > 1$ (parallel algorithm) is based on the non-parallel PISPMHAs. For example, the proposed approach with $\mathcal{T}_{\text{WJ}}$– $\mathcal{T}_{\text{GS}}$ is the same as the proposed approach with $\mathcal{T}_{\text{GS}}$ and the proposed approach with $\mathcal{T}_{\text{WJ}}$–$\mathcal{T}_{\text{SOR}}$, $\mathcal{T}_{\text{GS}}$–$\mathcal{T}_{\text{SOR}}$ and $\mathcal{T}_{\text{WJ}}$– $\mathcal{T}_{\text{GS}}$–$\mathcal{T}_{\text{SOR}}$ are the same as the proposed approach with $\mathcal{T}_{\text{SOR}}$. As a result that the parallel algorithm in which the $\mathcal{T}_{\text{SOR}}$ is used as its partial components (The proposed approach with $\mathcal{T}_{\text{WJ}}$–$\mathcal{T}_{\text{SOR}}$, $\mathcal{T}_{\text{GS}}$–$\mathcal{T}_{\text{SOR}}$, $\mathcal{T}_{\text{WJ}}$– $\mathcal{T}_{\text{GS}}$–$\mathcal{T}_{\text{SOR}}$), it will be give us the best convergence.

Next, Figures 3 and 4 show the average CPU time on each iteration and the CPU time consumption through out the process for WJ, GS, SOR and all cases studies of the PISPMHA in solving linear system (4.20) with $l = 50$, $l = 100$ and $l = 150$, respectively.

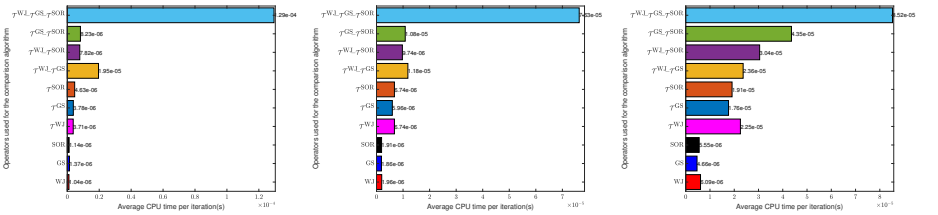

FIGURE 3. The average CPU time on each iteration for the suggested approach to problem to problem (4.19) with $l = 50$, $l = 100$ and $l = 150$, respectively.

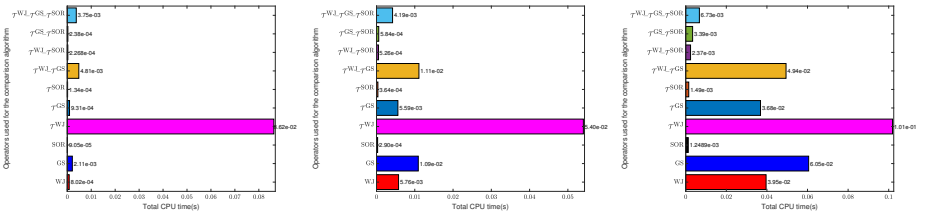

FIGURE 4. The CPU time consumption through out the process for the suggested approach to problem (4.20) with $l = 50$, $l = 100$ and $l = 150$ respectively.

It can be seen that the proposed approach with $\mathcal{T}_{\text{WJ}}-\mathcal{T}_{\text{GS}}-\mathcal{T}_{\text{SOR}}$ takes the most average of time per step of iteration. The SOR method takes the least time to complete the process. However, if we considering from the time consumption throughout the process the parallell methods in which the $\mathcal{T}_{\text{SOR}}$ is used as its partial components, the PISPMHA with $\mathcal{T}_{\text{WJ}}-\mathcal{T}_{\text{SOR}}$, $\mathcal{T}_{\text{GS}}-\mathcal{T}_{\text{SOR}}$ and $\mathcal{T}_{\text{WJ}}-\mathcal{T}_{\text{GS}}-\mathcal{T}_{\text{SOR}}$ will be no less interesting than others methods. Specifically, the proposed approach using $\mathcal{T}_{\text{WJ}}-\mathcal{T}_{\text{GS}}-\mathcal{T}_{\text{SOR}}$ which creates from all considered techniques comprises of WJ, GS, and SOR methods. We don't have to worry about which way achieves the fastest convergence; we simply choose all methods and then generate parallel suggested methods from them.

4.2. **Differential problems.** Let consider the following simple and well known one-dimensional heat equation with Dirichlet boundary conditions and initial data,

$$\begin{aligned} u_t &= \nu u_{xx} + f(x,t), \quad 0 < x < l, \quad t > 0. \\ u(x,0) &= u_0(x), \quad 0 < x < l, \end{aligned} \tag{4.23}$$

$$u(0,t) = \psi_1(t), \quad u(l,t) = \psi_2(t), \quad t > 0,$$

where ν is constant, $u(x,t)$ represents the temperature at point (x,t) and $f(x,t)$, $\psi_1(t)$, $\psi_2(t)$ are sufficiently smooth functions. Below, we use the notations u_i^n and $(u_{xx})_i^n$ to represent the numerical approximations of $u(x_i,t^n)$ and $u_{xx}(x_i,t^n)$ and $t^n = n\Delta t$, where Δt denotes the temporal mesh size. A set of schemes in solving problem (4.23) is based on the following well-known Crank-Nikolson type of scheme [40, 41],

$$\frac{u_i^{n+1} - u_i^n}{\Delta t} = \frac{\nu}{2}\left[(u_{xx})_i^{n+1} + (u_{xx})_i^n\right] + f_i^{n+1/2}, \quad i = 2, \ldots, N-1$$

with initial data

$$u_i^0 = u^0(x_i), \quad i = 2, \ldots, N-1$$

and Dirichlet boundary conditions

$$u_1^{n+1} = \psi_1(t^{n+1}), \quad u_N^{n+1} = \psi_2(t^{n+1}).$$

To approximate term of $(u_{xx})_i^k, k = n, n+1$, we use the standard centered discretization with space. The matrix form of second-order finite difference scheme (FDS) in solving heat problem (4.23) can be written as

$$A\mathbf{u}^{n+1} = \mathbf{G}^n, \tag{4.24}$$

where $\mathbf{G}^n = B\mathbf{u}^n + \mathbf{f}^{n+1/2}$,

$$A = \begin{bmatrix} 1+\alpha & -\frac{\alpha}{2} & & & \\ -\frac{\alpha}{2} & 1+\alpha & -\frac{\alpha}{2} & & \\ & \ddots & \ddots & \ddots & \\ & & -\frac{\alpha}{2} & 1+\alpha & -\frac{\alpha}{2} \\ & & & -\frac{\alpha}{2} & 1+\alpha \end{bmatrix}, \quad B = \begin{bmatrix} 1-\alpha & \frac{\alpha}{2} & & & \\ \frac{\alpha}{2} & 1-\alpha & \frac{\alpha}{2} & & \\ & \ddots & \ddots & \ddots & \\ & & \frac{\alpha}{2} & 1-\alpha & \frac{\alpha}{2} \\ & & & \frac{\alpha}{2} & 1-\alpha \end{bmatrix},$$

$$\mathbf{u}^n = \begin{bmatrix} u_2^k \\ u_3^k \\ \vdots \\ u_{N-2}^k \\ u_{N-1}^k \end{bmatrix}, \quad \mathbf{f}^{n+1/2} = \begin{bmatrix} \frac{\alpha}{2}\psi_1^{n+1/2} + \Delta t f_2^{n+1/2} \\ \Delta t f_3^{n+1/2} \\ \vdots \\ \Delta t f_{N-2}^{n+1/2} \\ \frac{\alpha}{2}\psi_2^{n+1/2} + \Delta t f_{N-1}^{n+1/2} \end{bmatrix},$$

$\alpha = \nu\Delta t/\left(\Delta x^2\right)$, $\psi_i^{n+1/2} = \psi_i(t^{n+1/2}), i = 1, 2$ and $f_i^{n+1/2} = f_i(t^{n+1/2}), i = 2, \ldots, N-1$.

From equation (4.24), matrix A is square and symmetric positive definite. Traditionally iterative methods have been presented in solving the solution of linear systems (4.24). The well-known weight Jacobi (WJ), successive over relaxation (SOR) and Gauss-Seidel (GS, SOR with $\omega = 1$) methods [19, 40] are chosen to exemplify here (see on Table 3).

Linear system	Iterative method	Specific name
$A\mathbf{u}^{n+1} = \mathbf{G}^n$	$D\mathbf{u}^{(n+1,s)} = (D - \omega A)\,\mathbf{u}^{(n+1,s)} + \omega\mathbf{G}^n$	WJ
	$(D - \omega L)\,\mathbf{u}^{(n+1,s)} = \Big((D - \omega L) - \omega A\Big)\mathbf{u}^{(n+1,s)} + \omega\mathbf{G}^n$	SOR

TABLE 3. The specific name of WJ and SOR in solving linear system (4.24).

The implemented of WJ and SOR methods in solving the solution of linear systems (4.24) can bee seen on [15]. And ω is weight parameter, D is the diagonal part of matrix A and L is the lower triangular part of matrix $D - A$, respectively. Moreover, the optimal weight parameter ω_o are also indicated with the same formula on Table 2. For stability of WJ and SOR method in solving linear system (4.24) generates from the discretization of the consideration problem (4.23), the step sizes of time play an important role of the stability needed. The discussion on the stability of WJ and SOR in solving linear system (4.24) can be found in [19, 40].

Since the well-known WJ, SOR and Gauss-Seidel (GS, SOR with $\omega = 1$) methods in solving linear system (4.24) can be presented in the form of fixed point equation as $\mathcal{T}_{\text{WJ}}(\mathbf{u}) = \mathbf{u}$, $\mathcal{T}_{\text{SOR}}(\mathbf{u}) = \mathbf{u}$ and $\mathcal{T}_{\text{GS}}(\mathbf{u}) = \mathbf{u}$, respectively then we introduce a new iterative method using the G-nonexpansive mapping $\mathcal{T}_i, \forall i = 1, 2, \ldots, M$. The generated sequence $\{\mathbf{u}^n\}$ for a new PISPMHA is created iteratively by using two initial data $\mathbf{u}^{(n,0)}, \mathbf{u}^{(n,1)} \in \mathbb{R}^l$ and

$$
\begin{aligned}
\mathbf{w}^{(n,s)} &= \mathbf{u}^{(n,s)} + \theta_n \left(\mathbf{u}^{(n,s)} - \mathbf{u}^{(n,s-1)}\right), \\
\mathbf{z}_i^{(n,s)} &= (1-\gamma_i^s)\mathbf{w}^{(n,s)} + \gamma_i^s \mathcal{T}_i \mathbf{w}^{(n,s)}, \\
\mathbf{y}_i^{(n,s)} &= (1-\beta_i^s)\mathbf{z}_i^{(n,s)} + \beta_i^s \mathcal{T}_i \mathbf{z}_i^{(n,s)}, \\
\mathbf{h}_i^{(n,s)} &= (1-\alpha_i^s)\mathbf{y}_i^{(n,s)} + \alpha_i^s \mathcal{T}_i \mathbf{y}_i^{(n,s)},\ n \geq 0, \\
\mathbf{u}^{(n+1,s)} &= \text{argmax}\left\{||\mathbf{h}_i^{(n,s)} - \mathbf{w}^{(n,s)}||, i = 1, 2, \ldots, M\right\},
\end{aligned}
\tag{4.25}
$$

where the second superscript "s" denotes the number of iterations $s = 1, 2, \ldots, \widehat{S}_n$ and set

$$
\gamma_i^s = \frac{s}{s+1}, \quad \beta_i^s = \gamma_i^s, \quad \alpha_i^s = \gamma_i^s,
$$

and $\{\theta_n\}$ is set as equation (4.22). The nonexpansive mapping $\mathcal{T}_i$ of the PISPMHA can be chosen from these three operators $\mathcal{T}_{\text{GS}}, \mathcal{T}_{\text{WJ}}$ and $\mathcal{T}_{\text{SOR}}$. And we call the PISPMHA as a parallel algorithm if $M \geq 2$ is chosen. The step size of time for the PISPMHA are based on the smallest step size chosen from WJ, GS and SOR method in solving linear system (4.24) generated from the discretization of the consideration problem (4.23).

In all computations, we used $\nu = 25$, $\Delta t = \Delta x^2/10$ (step size of time) and $\epsilon_d = 10^{-10}$. For testing purpose only, both computations are performed for $0 \leq t \leq 0.01$ (when $t \gg 0.05, u(x,t) \to 0$). The following stopping criterion is used

$$
\|\mathbf{u}^{(n+1,\widehat{S}_n)} - \mathbf{u}^{(n+1,\widehat{S}_{n-1})}\|_2 < \epsilon_d,
$$

where "$\widehat{S}_n$" denotes the number of the last iteration at time $\mathcal{T}_n$ and after that set

$$
\mathbf{u}^{(n,0)} = \mathbf{u}^{(n+1,\widehat{S}_{n-1})} \quad \text{and} \quad \mathbf{u}^{(n,1)} = \mathbf{u}^{(n+1,\widehat{S}_n)}.
$$

All computations are performed by using uniform grid of 161 nodes which corresponds to the solution of linear systems (4.24) with 159×159 sizes respectively. We apply the WJ, SOR, GS and the PISPMHA with parallel and non-parallel cases of these three operators $\mathcal{T}_{\text{GS}}, \mathcal{T}_{\text{WJ}}$ and $\mathcal{T}_{\text{SOR}}$ in getting the solution of linear system (4.24) of heat problem with Dirichlet boundary conditions and initial data (4.23).

Let consider the following heat problem:

$$
\begin{aligned}
&u_t = \nu u_{xx} + 0.4\nu(4\pi^2 - 1)e^{-4\nu t}\cos(4\pi x), \quad 0 \leq x \leq 1, \quad 0 < t < t_s, \\
&u(x,0) = \cos(4\pi x)/10, \quad u(0,t) = e^{-4\nu t}/10, \quad u(1,t) = e^{-4\nu t}/10, \\
&u(x,t) = e^{-4\nu t}\cos(4\pi x)/10.
\end{aligned}
\tag{4.26}
$$

The results of the basic iterative methods (WJ, GS, SOR) and the PISPMHA with the operators $\mathcal{T}_{\text{GS}}, \mathcal{T}_{\text{WJ}}$ and $\mathcal{T}_{\text{SOR}}$ similar to the previous section are demonstrated and discussed.

The relative error on each step of time are measured by using the following formula

$$
\|\mathbf{u}^{n+1} - \mathbf{u}^{(n+1,\widehat{S}_n)}\|_2 / \|\mathbf{u}^{n+1}\|_2.
$$

The trend of the average iterations number for the fundamental iterative methods is shown in Figure 5 compared to all cases of the suggested algorithms in addressing the discretization of consideration issue (4.26) with different grid sizes.

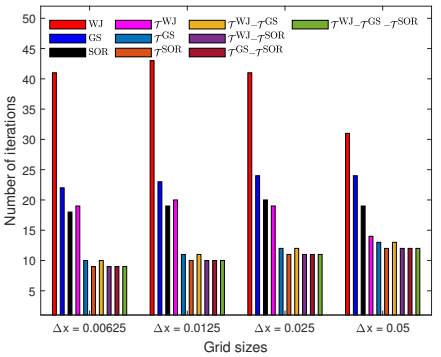

FIGURE 5. The evolution of the average iterations number on each step of time for GS, WJ, SOR and the suggested method to problem (4.23).

It can be seen from this figure that the average number of iteration on each step of time for the PISPMHA with $M > 1$ is smaller than the basic iterative methods. Furthermore, for all of the consideration grid sizes, the average number of iterations on each step of time for the suggested method in which the operator $\mathcal{T}_{\text{SOR}}$ is utilized as one of its partial components gives us the smallest number of iterations.

Since the PISPMHA is designed using all consideration methods, regardless of which method gives us the fastest convergence discussed in the previous section. The PISPMHA with $\mathcal{T}_{\text{WJ}}$–$\mathcal{T}_{\text{GS}}$–$\mathcal{T}_{\text{SOR}}$ is chosen to test and verify the order of accuracy for the presented FDS in solving heat equation (4.26). And, for all computations, uniform grids of $11, 21, 41, 81$ and 161 nodes are used, which correspond to the discretization of heat equation problem (4.26) with $\Delta x = 0.1, 0.05, 0.025, 0.0125, 0.0625$, respectively.

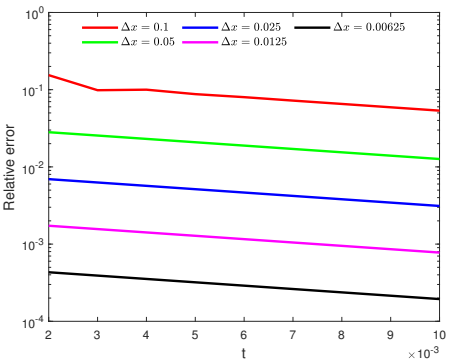

FIGURE 6. The evolution of relative error in getting the numerical solution of problem (4.26) with various grid sizes by using the suggested method with $\mathcal{T}_{\text{WJ}}$–$\mathcal{T}_{\text{GS}}$–$\mathcal{T}_{\text{SOR}}$.

It can be seen from Figure 6 that the PISPMHA with $\mathcal{T}_{\text{WJ}}$–$\mathcal{T}_{\text{GS}}$–$\mathcal{T}_{\text{SOR}}$ are seen to be second order of accuracy. That is the order of accuracy of the PISPMHA with $\mathcal{T}_{\text{WJ}}$–$\mathcal{T}_{\text{GS}}$–$\mathcal{T}_{\text{SOR}}$ agrees with their FDS construction.

Next, we compare the PISPMHA's convergence behavior and performance to the basic iterative technique for problem (4.26) with $\nu = 25$ and $t \in (0, 1]$ when the grid sizes are

set with 161 nodes. The estimated solution of problem (4.26) at $t = 0.01$ using the basic iterative approach and the PISPMHA with $M \leq 3$ is shown in Figure 7.

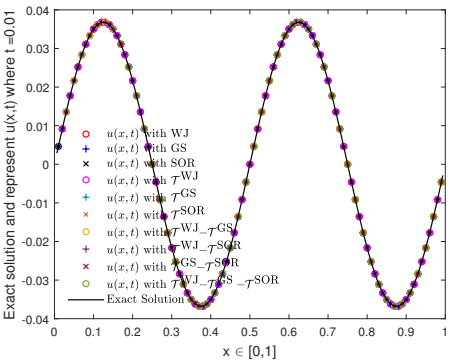

FIGURE 7. Approximate solutions of the basic iterative methods and the suggested method.

The trend of iterations number for the basic iterative methods and the suggested algorithm in solving problem (4.24) originates from the discretization of the consideration problem (4.26) with 161 nodes is shown in Figure 8. In comparison to the basic iterative methods, the suggested method with parallel case needs fewer iterations on each step of time, as shown in Figure 8. And the recommended approaches that use the operator $\mathcal{T}_{SOR}$ as partial components provide us the fewest number of iterations at each time step.

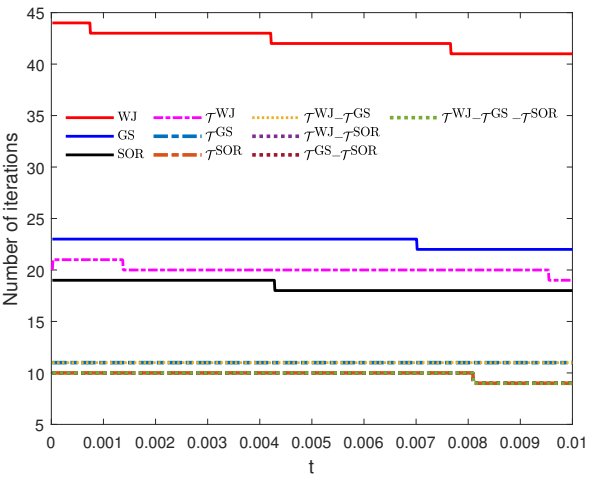

FIGURE 8. The evolution of iterations number for the basic iterative methods and the suggested method.

The average CPU time on each iteration and CPU time consumption throughout the process for WJ, GS, SOR, and all case studies of the proposed approach in addressing the consideration problem (4.26) with 161 nodes are shown in Figure 9. The suggested method with the parallel situation always takes the longest average time per iteration

step. On the other hand, the fundamental iterative method takes the shortest time to finish the procedure. However, with parallel situations, examine the time consumption of the suggested method throughout the procedure. It will take not much different time when compared to the WJ approach.

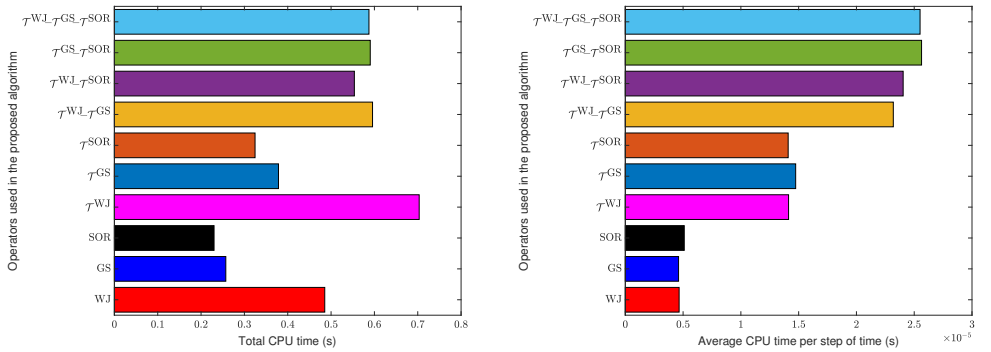

FIGURE 9. The average CPU time on each iteration and the CPU time consumption through out the process for the basic iterative methods and the suggested method.

4.3. **Signal recovering.** The minimization problem of the sum of two functions is to find a solution of

$$\min_{\mathbf{x}\in\mathbb{R}^n}\{F(\mathbf{x}) := f(\mathbf{x}) + g(\mathbf{x})\}, \tag{4.27}$$

where $g : \mathbb{R}^n \to \mathbb{R} \cup \{\infty\}$ is proper convex and lower semi-continuous function, and $f : \mathbb{R}^n \to \mathbb{R}$ is convex differentiable function with gradient ∇f being L-Lipschitz constant for some $L > 0$. The solution of (4.27) can be characterized by using Fermat's rule, Theorem 16.3 of Bauschke and Combettes [10] as follows:

$$\mathbf{x}^* \text{ is a minimizer of } (f+g) \;\Leftrightarrow\; 0 \in \partial g(\mathbf{x}^*) + \nabla f(\mathbf{x}^*),$$

where ∂g is the subdifferential of g and ∇f is the gradient of f. The subdifferential of g at $\mathbf{x}^*$, denoted by $\partial g(\mathbf{x}^*)$, is defined by

$$\partial g(\mathbf{x}^*) := \{u : g(\mathbf{x}) - h(\mathbf{x}^*) \geq \langle u, \mathbf{x} - \mathbf{x}^*\rangle\,,\ \forall \mathbf{x}\}.$$

Additionally, it is generally known that the following fixed point problem characterizes the solution of (4.27):

$$\mathbf{x}^* \text{ is a minimizer of } (f+g) \;\Leftrightarrow\; \mathbf{x}^* = prox_{\tau g}(I - \tau\nabla f)(\mathbf{x}^*),$$

where $\tau > 0, prox_g$ is the proximity operator of h defined by $prox_g := argmin\{g(\mathbf{y}) + \frac{1}{2}\|\mathbf{x}-\mathbf{y}\|_2^2\}$, see [26] for more details. It is also known that $prox_{\tau g}(I - \tau\nabla f)$ is a nonexpansive mapping when $\tau \in \left(0, \frac{2}{L}\right)$.

Next, we apply the PISPMHAs to solve the signal recovering problems. In signal processing, compressed sensing can be modeled as the following under determinated linear equation system

$$\mathbf{y} = A\mathbf{x} + n,$$

where $A \in \mathbb{R}^{m\times n}$ is a degraded matrix, $\mathbf{x} \in \mathbb{R}^n$ is an original signal with n components to be recovered and $n, \mathbf{y} \in \mathbb{R}^m$ are noise and the observed signal with noisy for m components respectively. Finding the solutions of previous determinated linear equation system

can be seen as solving the LASSO problem

$$\min_{\mathbf{x}\in\mathbb{R}^N} \frac{1}{2}\|\mathbf{y}-A\mathbf{x}\|_2^2+\lambda\|\mathbf{x}\|_1, \tag{4.28}$$

where $\lambda>0$. As a result various techniques and iterative schemes have been developed to solve the Lasso problem. We can apply the minimization problem of the sum of two functions for solving the LASSO problem (4.28) by setting

$$S(\mathbf{x}) = prox_{\tau h}\left(\mathbf{x}-\tau\nabla f(\mathbf{x})\right),$$

where $f(\mathbf{x})=\|\mathbf{y}-A\mathbf{x}\|_2^2/2$, $h(x)=\lambda\|\mathbf{x}\|_1$, $\nabla f(\mathbf{x})=A^T(A\mathbf{x}-\mathbf{y})$.

Now, we present the parallel iterative method in recovering the original signal $\mathbf{x}$ when the observed signals $\mathbf{y}_1,\mathbf{y}_2,...,\mathbf{y}_M$ can be recovered by using the degraded matrices A_1, A_2, ..., A_M, repectively in which

$$\mathbf{y}_i = A_i\mathbf{x}+n_i, i=1,2,\ldots,M. \tag{4.29}$$

That is, the original signal $\mathbf{x}$ is a common solution of the M-determinated system of linear equations (4.29). Let us consider the following M-LASSO problems which is called as the LASSO system introduced by Suantai et al. [36]:

$$\begin{aligned}
&\min_{\mathbf{x}\in\mathbb{R}^N} \frac{1}{2}\|A_1\mathbf{x}-\mathbf{y}_1\|_2^2+\lambda_1\|\mathbf{x}\|_1,\\
&\min_{\mathbf{x}\in\mathbb{R}^N} \frac{1}{2}\|A_2\mathbf{x}-\mathbf{y}_2\|_2^2+\lambda_2\|\mathbf{x}\|_1,\\
&\qquad\qquad\vdots\\
&\min_{\mathbf{x}\in\mathbb{R}^N} \frac{1}{2}\|A_M\mathbf{x}-\mathbf{y}_M\|_2^2+\lambda_M\|\mathbf{x}\|_1,
\end{aligned} \tag{4.30}$$

where the original signal $\mathbf{x}$ is common solution of LASSO system (4.30). We will find the true signal $\mathbf{x}$ through the common solution of LASSO system. Let

$$\mathcal{S}_i(\mathbf{x}) = prox_{\tau_i g_i}\big(\mathbf{x}+\tau_i A_i^t(A_i\mathbf{x}-\mathbf{y}_i)\big).$$

We apply the PISPMHA in finding the common solution $\mathbf{x}$ for the LASSO system:

$$\begin{aligned}
\mathbf{w}_n &= \mathbf{x}_n+\theta_n(\mathbf{x}_n-\mathbf{x}_{n-1})\\
\mathbf{z}_n^i &= (1-\gamma_n^i)\mathbf{w}^n+\gamma_n^i\mathcal{S}_i(\mathbf{w}^n),\\
\mathbf{y}_n^i &= (1-\beta_n^i)\mathbf{z}_n^i+\beta_n^i\mathcal{S}_i(\mathbf{z}_n^i),\\
\mathbf{h}_n^i &= (1-\alpha_n^i)\mathbf{y}_n^i+\alpha_n^i\mathcal{S}_i(\mathbf{y}_n^i),\\
\mathbf{x}_{n+1} &= \text{argmax}\left\{||\mathbf{h}_n^i-\mathbf{w}_n||, i=1,2,\ldots,M\right\},
\end{aligned} \tag{4.31}$$

where $g_i(\mathbf{x})=\lambda_i\|\mathbf{x}\|_1$, $\tau_i=2/\|A_i^TA_i\|_2$, the default parameters θ_n and $\{\alpha_n^i\},\{\beta_n^i\},\{\gamma_n^i\}$ are set as equations (4.21) and (4.22). And, we called the algorithm (4.31) as the PISPMHA with degraded matrices $A_i, i=1\ldots M$.

Next, some experiments are provided to illustrate the convergence and the effectiveness of the PISPMHA (4.31) and compare with the FISTA algorithm [11], Suantai et al. [36], Cholamjiak et al. [16] and Jun-on et al. [23]. The original signal x with $n=1024$ generated by the uniform distribution in the interval $[-2,2]$ with 70 nonzero elements is used to create the observation signal with $m=512$ and $\mathbf{y}_i=A_i\mathbf{x}+n_i$ where $j\leq 3$.

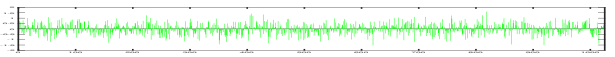

FIGURE 10. Original Signal (x) with $m = 70$.

The observation signal $\mathbf{y}_i, i = 1, 2, 3$ show on Figure 11.

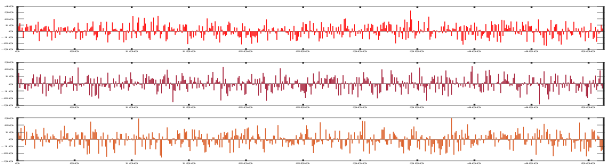

FIGURE 11. Degraded Signals $\mathbf{y}_1$, $\mathbf{y}_2$, and $\mathbf{y}_3$, respectively.

The matrices A_i generated by the normal distribution with mean zero and variance one and the white Gaussian noise $\mathbf{n_i}$ (see on Figure 12).

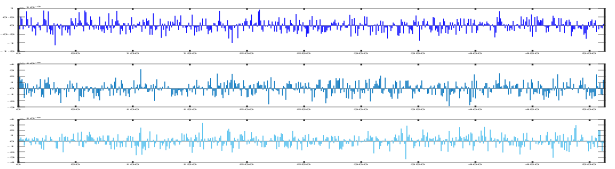

FIGURE 12. Noise Signals $\mathbf{n}_1$, $\mathbf{n}_2$, and $\mathbf{n}_3$, respectively.

Both theoretical and experimental results for the convergence properties of the PISPMHA with the permutation of the blurring matrices A_1, A_2 and A_3 are demonstrated and discussed on the following cases:

Case I: The PISPMHA with $\mathcal{S}_1$.
Case II: The PISPMHA with $\mathcal{S}_2$.
Case III: The PISPMHA with $\mathcal{S}_3$.
Case IV: The PISPMHA with $\mathcal{S}_1$–$\mathcal{S}_2$.
Case V: The PISPMHA with $\mathcal{S}_1$–$\mathcal{S}_3$.
Case VI: The PISPMHA with $\mathcal{S}_2$–$\mathcal{S}_3$.
Case VII: The PISPMHA with $\mathcal{S}_1$–$\mathcal{S}_2$–$\mathcal{S}_3$.

The process is started when the signal initial data $\mathbf{x}_0$ and $\mathbf{x}_1$ with $n = 1024$ is picked randomly.

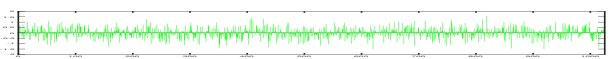

Initial Signal ($\mathbf{x}_0$)

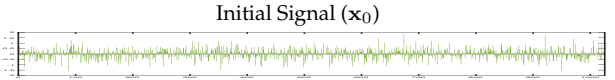

Initial Signal ($\mathbf{x}_1$)

FIGURE 13. Initial Signals $\mathbf{x}_0$ and $\mathbf{x}_1$.

The relative signal error is measured by the following formula

$$\|\mathbf{x}_n - \mathbf{x}\|_2 / \|\mathbf{x}\|_2$$

in order to check the convergence of all comparative algorithms. The signal-to-noise ratio (SNR), which is defined as

$$\mathrm{SNR}(\mathbf{x}_n) = 20 \log_{10} \left(\frac{\|\mathbf{x}_n\|_2}{\|\mathbf{x}_n - \mathbf{x}\|_2} \right),$$

is used to evaluate a signal quantitatively, $\mathbf{x}_n$ is the signal recovered at iteration n^{th} using the proposed approach.

Figures 14 and Figure 15 show the signal relative error and SNR quality of all comparing methods for recovering the degraded signal.

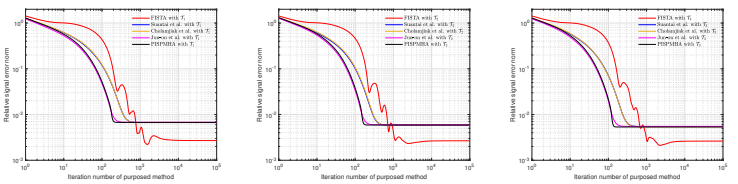

Non-Parallell situation (PISPMHA with case I-III).

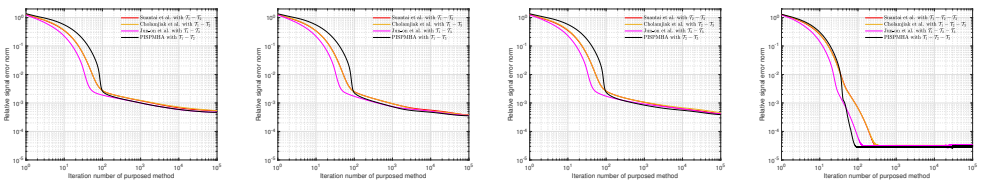

Parallell situation (PISPMHA with case IV-VII).

FIGURE 14. The relative error norm of all comparative methods.

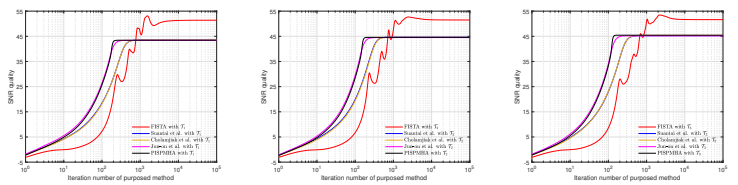

Non-Parallell situation (PISPMHA with case I-III).

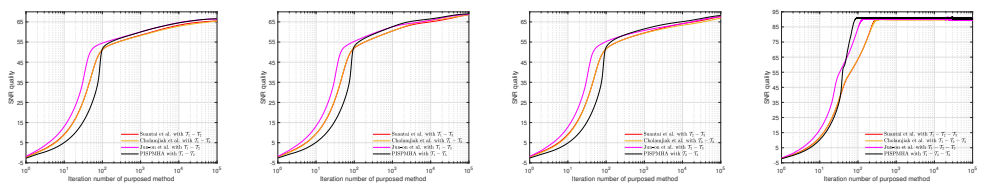

Parallell situation.

FIGURE 15. The SNR plots of all comparative methods (PISPMHA with case IV-VII).

Figure 14 shows that the relative error plots of all algorithms are decreased as the iteration number increases and after that they converge to some constants. The relative errors plot demonstrates the validity of all comparative algorithms and confirms their convergence. The first three figures of Figure 14 show that when the number of iterations is lagge enough, the FISTA method provides us the least relative error. It should also be highlighted that within the first 500 iterations, the PISPMHA and Jun-on et al. methods approaches converge similarly and faster than the other comparable methods. With the exception of FISTA techniques, the remaining figures of Figure 14 depict the convergence behavior of all comparison approaches (all methods that can be parallel computing). The other parallel approaches converge significantly better than the proposed method, as can be seen. However, after 100 iterations the proposed method converges better.

Figure 15 shows that the SNR quality of the restored signal using all comparative methods increases until it converges to some constant value. The FISTA method outperforms the other approaches when the quality of the recovered signal is attained using only one of the dregraded matrices, as seen in the first three figures of Figure 15. The remaining figures of Figure 15 show the SNR quality of all comparative methods excepted FISTA methods. It can be seen that the SNR quality of the restored image for all parallel algorithms are improved and better than FISTA method. And, when all degrading matrices is used in finding the common solutions of the signal recovering problem, we get the best quality of the recovering signal. With the exception of FISTA techniques, the remaining figures of Figure 15 illustrate the SNR quality of all comparing methods. All parallel methods improve and outperform the FISTA method in terms of SNR quality of the restored image. We acquire the best quality of the recovered signal when all degrading matrices are applied in discovering the common solutions of the signal recovering challenge.

Figure 16 displays the SNR plots for the best case of FISTA technique and all comparative parallel methods that use all degradation matrices within 100^{th} iterations. We discovered that all parallel approaches outperform the FISTA method in terms of quality. And, after 50 iterations, the PISPMHA approach provides us the best quality. Moreover, the highest SNR quality can be achieved within the first 100 iterations.

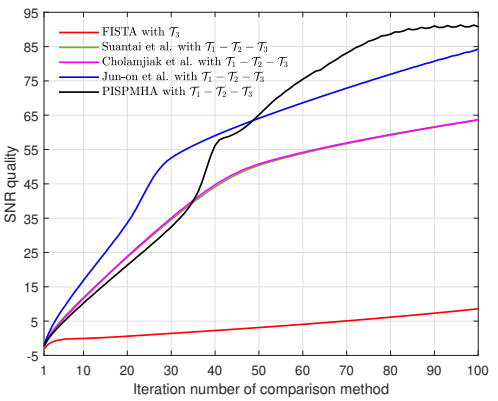

FIGURE 16. The SNR plots of FISTA method and all comparative parallel methods in which all degrading matrices within 100^{th} iterations.

Next, the average CPU time on each iteration and the CPU time usage throughout the operation within 100 iterations are then displayed for all comparative methodologies. Figures 17 and 18 show that the proposed technique, which uses all degradation matrices,

takes the longest average time on each iteration step and also consumes the greatest CPU time during the procedure. That's the one of the disadvantage of the proposed method.

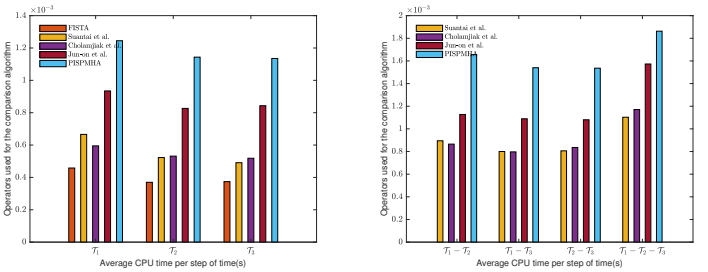

FIGURE 17. The CPU time consumption through out the process for FISTA and all parallel methods within 100^{th} iterations.

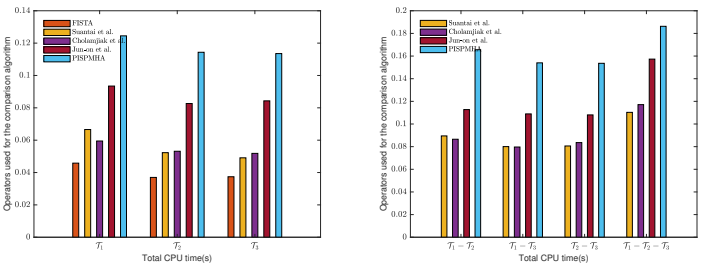

FIGURE 18. The CPU time consumption through out the process for FISTA and all parallel methods within 100^{th} iterations.

The last figure shows the best quality of the restored signals at 90^{th} step of iterations for all comparative methods.

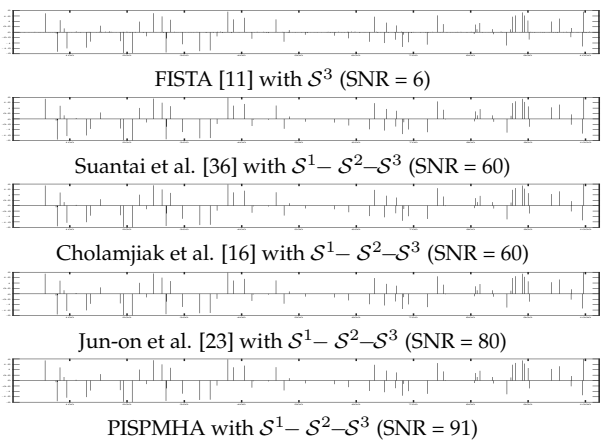

FIGURE 19. Recovering signals being used the FISTA method and all comparative parallel methods in which all degrading matrices at 90^{th} iterations.

5. Conclusions

In this article, we achieve the parallel inertial SP-iteration monotone hybrid algorithm (PISPMHA) to solve a common fixed point of a finite family of G-nonexpansive mappings on Hilbert spaces involving a graph. We have proved weak convergence of the sequence generated by above said algorithm to an element of the problem's solution set under some certain conditions. As applications, we give the idea how to apply fundamental iterative methods like WJ, GS, and SOR to the proposed approach in with parallel and non-parallel cases in solving the unique solution of the differential problems. The suggested method converges to precise answers for all considered issues. The proposed methods, which apply WJ, GS, and SOR techniques to our algorithm, demonstrate that we don't need to worry about which approach provides the fastest convergence; instead, we may pick all methods and construct parallel recommended ways from them. And, for the parallel algorithm, the number of iterations is determined by the fastest fundamental method that is developed as one of its partial components. Furthermore, we discovered that, when compared to the FISTA technique, the suggested approach with the parallel case extends the quality range of the recovered signal when applied to the common solution of signal recovery difficulties. When all degrading matrices are used to find the common solutions to the signal recovery challenge, the recovered signal has the best quality. One of the downsides of the proposed method applying differential and signal recovering problems is the longest average time on each iteration step compared with other methods.

Acknowledgments This research was supported by University of Phayao and Thailand Science Research and Innovation Fund (Fundamental Fund 2024).

References

[1] Aleomraninejad, S. M. A.; Rezapour, S.; Shahzad, N. Some fixed point result on a metric space with a graph. *Topol. Appl.* **159** (2012), 659–663. https://doi.org/10.1016/j.topol.2011.10.013.

[2] Alfuraidan, M. R. Fixed points of monotone nonexpansive mappings with a graph. *Fixed Point Theory Appl.* **49** (2015), https://doi.org/10.1186/s13663-015-0299-0.

[3] Alfuraidan, M. R.; Khamsi, M. A. Fixed points of monotone nonexpansive mappings on a hyperbolic metric space with a graph. *Fixed Point Theory Appl.* **44** (2015), https://doi.org/10.1186/s13663-015-0294-5.

[4] Alvarez, F.; Attouch, H. An inertial proximal method for maximal monotone operators via discretization of a nonlinear oscillator with damping. *Set-Valued Analysis* **9** (2001), 3–11. https://doi.org/10.1023/A:1011253113155.

[5] Anh, P. K.; Hieu, D. V. Parallel and sequential hybrid methods for a finite family of asymptotically quasi -nonexpansive mappings. *J. Appl. Math. Comput.* **48** (2015), 241–263. https://doi.org/10.1007/s12190-014-0801-6.

[6] Anh, P. K.; Hieu, D. V. Parallel Hybrid Iterative Methods for Variational Inequalities, Equilibrium Problems, and Common Fixed Point Problems. *Vietnam J. Math.* **44** (2016), 351–374. https://doi.org/10.1007/s10013-015-0129-z.

[7] Asl, J. H.; Mohammadi, B.; Rezapour, S.; Vaezpour, S. M. Some fixed point results for generalized quasi-contractive multifunctions on graphs. *Filomat* **27** (2013), no. 2, 311–315.

[8] Attouch, H.; Peypouquet, J.; Redont, P. A dynamical approach to an inertial forward-backward algorithm for convex minimization. *SIAM J. Optimiz.* **24** (2014), 232–256. https://doi.org/10.1137/130910294.

[9] Banach, S. Sur les oprations dans les ensembles abstraits et leur application aux quations intgrales. *Fund. Math.* **3** (1922), 133–181.

[10] Bauschke, H. H.; Combettes, P. L. *Convex Analysis and Monotone Operator Theory in Hilbert Spaces*. 243 2nd ed. Incorporated, Springer, New York, NY, USA, 2017.

[11] Beck, A.; Teboulle, M. A fast iterative shrinkage-thresholding algorithm for linear inverse problems. *SIAM J. Imaging Sci.* **2** (2009), no. 1, 183–202.

[12] Bojor, F. Fixed point of ϕ-contraction in metric spaces endowed with a graph. *Ann. Univ. Craiova Math. Ser.Mat. Inform.* **37** (2010), 85–92.

[13] Bojor, F. Fixed point theorems for Reich type contractions on metric spaces with a graph. *Nonlinear Anal.* **75** (2012), 3895–3901. https://doi.org/10.1016/j.na.2012.02.009.

[14] Bojor, F. Fixed points of Kannan mappings in metric spaces endowed with a graph. *An. St. Univ. Ovidius Constanta Ser. Mat.* **20** (2012), 31–40.
[15] Charoensawan, P.; Yambangwai, D.; Cholamjiak W.; Suparatulatorn R. An inertial parallel algorithm for a finite family of G-nonexpansive mappings with application to the diffusion problem. *Adv Differ. Equ.* **453** (2021), https://doi.org/10.1186/s13662-021-03613-4.
[16] Cholamjiak, W.; Khan, S. A.; Yambangwai, D.; Kazmi, K. R. Strong convergence analysis of common variational inclusion problems involving an inertial parallel monotone hybrid method for a novel application to image restoration . *RACSAM* **114** (2020), no. 99, 1—20. https://doi.org/10.1007/s13398-020-00827-1.
[17] Chonjaroen, C.; Yambangwai, D.; Thianwan, T. New iterative methods for nonlinear operators as concerns convex programming applicable in differential problems, image deblurring, and signal recovering problems. *Math. Meth. Appl. Sci.* **2022** (2022), 1–24. https://doi.org/10.1002/mma.8693.
[18] Glowinski, R.; Tallec, P. L. *Augmented Lagrangian and Operator-Splitting Methods in Nonlinear Mechanic.* SIAM, Philadelphia, 1989.
[19] Grzegorski, S. M. On Optimal Parameter Not Only for the SOR Method. *Applied and Computational Mathematics* **8** (2019), no. 5, 82–87. doi: 10.11648/j.acm.20190805.11.
[20] Haubruge, S.; Nguyen, V. H.; Strodiot, J. J. Convergence analysis and applications of the Glowinski-Le Tallec splitting method for finding a zero of the sum of two maximal monotone operators. *J. Optim. Theory Appl.* **97** (1998), 645–673. https://doi.org/10.1023/A:1022646327085.
[21] Jachymski, J. The contraction principle for mappings on a metric space with a graph. *Proc. Amer. Math. Soc.* **136** (2008), no. 4, 1359–1373.
[22] Johnsonbaugh, R. *Discrete Mathematics.* New Jersey, 1997.
[23] Jun-on, N.; Suparatulatorn, R.; Gamal, M.; Cholamjiak W. An inertial parallel algorithm for a finite family of G-nonexpansive mappings applied to signal recovery. *AIMS Mathematics* **7** (2021), no. 2, 1775–1790. doi: 10.3934/math.2022102.
[24] Kelisky, R. P.; Rivlin, T. J. Iterates of Bernstein polynomials. *Pacific J. Math.* **21** (1967), no. 3, 511–520.
[25] Maing, P. E. Regularized and inertial algorithms for common fixed points of nonlinear operators. ´ *J. Math. Anal. Appl.* **344** (2008), no. 2, 876–887. https://doi.org/10.1016/j.jmaa.2008.03.028.
[26] Moreau, J. J. Proximité et dualité dans un espace hilbertien. *Bull. Soc. Math. Fr.* **93** (1965), 273–299.
[27] Nicolae, A.; Regan, D. O.; Petrusel, A. Fixed point theorems for single-valued and multivalued generalized contractions in metric spaces endowed with a graph. *Georgian Math. J.* **18** (2011), no. 2, 307–327. https://doi.org/10.1515/gmj.2011.0019.
[28] Polyak, B. T. Some methods of speeding up the convergence of iterative methods, *USSR Comput. Math. Math. Phys.* **4** (1964), no. 5, 1–17. https://doi.org/10.1016/0041-5553(64)90137-5.
[29] Samreen, M.; Kamran, T. Fixed point theorems for integral G-contractions. *Fixed Point Theory Appl.* **149** (2013), https://doi.org/10.1186/1687-1812-2013-149.
[30] Tiammee, J.; Kaewkhao, A.; Suantai, S. On Browder's convergence theorem and Halpern iteration process for G-nonexpansive mappings in Hilbert spaces endowed with graphs. *Fixed Point Theory Appl.* **187** (2015), https://doi.org/10.1186/s13663-015-0436-9.
[31] Tiammee, J.; Suantai, S. Coincidence point theorems for graph-preserving multi-valued mappings. *Fixed Point Theory Appl.* **70** (2014), https://doi.org/10.1186/1687-1812-2014-70.
[32] Tripak, O. Common fixed points of G-nonexpansive mappings on Banach spaces with a graph. *Fixed Point Theory Appl.* **87** (2016), https://doi.org/10.1186/s13663-016-0578-4.
[33] Sridarat, P.; Suparaturatorn, R.; Suantai, S.; Cho, Y. J. Covergence analysis of SP-iteration for G-nonexpansive mappings with directed graphs. *Bull. Malays. Math. Sci. Soc.* **42** (2019), 2361–2380. https://doi.org/10.1007/s40840-018-0606-0.
[34] Suantai, S. Weak and strong convergence criteria of Noor iterations for asymptotically nonexpansive mappings. *J. Math. Anal. Appl.* **311** (2005), no. 2, 506–517. https://doi.org/10.1016/j.jmaa.2005.03.002.
[35] Suantai, S.; Donganont, M.; Cholamjiak, W. Hybrid methods for a countable family of G-nonexpansive mappings in Hilbert spaces endowed with graphs, *Mathematics* **7** (2019), no. 10, 936. https://doi.org/10.3390/math7100936.
[36] Suantai, S.; Kankam, K.; Cholamjiak, P.; Cholamjiak, W. A parallel monotone hybrid algorithm for a finite family of G-nonexpansive mappings in Hilbert spaces endowed with a graph applicable in signal recovery. Comp. Appl. Math. **145** (2021), 40. https://doi.org/10.1007/s40314-021-01530-6.
[37] Suparatulatorn, R.; Suantai, S.; Cholamjiak, W. Hybrid methods for a finite family of G-nonexpansive mappings in Hilbert spaces endowed with graphs. *AKCE Int. J. Graphs Co.* **14** (2017), no. 2, 101–111. https://doi.org/10.1016/j.akcej.2017.01.001.
[38] Thong, D. V.; Hieu, D. V. Inertial extragradient algorithms for strongly pseudomonotone variational inequalities. *J. Comput. Appl. Math.* **341** (2018), 80–98. https://doi.org/10.1016/j.cam.2018.03.019.
[39] Thong, D. V.; Van Hieu, D. Modified subgradient extragradient method for variational inequality problems. *Numer. Algor.* **79** (2018), 597–610. https://doi.org/10.1007/s11075-017-0452-4.

[40] Yambangwai, D.; Cholamjiak, W.; Thianwan, T.; Dutta, H. On a new weight tri-diagonal iterative method and its applications. *Soft Comput.* **25** (2021), 725–740. https://doi.org/10.1007/s00500-020-05181-3.
[41] Yambangwai, D.; Moshkin N. Deferred correction technique to construct high-order schemes for the heat equation with dirichlet and neumann boundary conditions. *Engineering Letters* **21** (2013), no. 2, 61–67.
[42] Zhang, L. Y.; Zhao, H.; Lv, Y. B. A modified inertial projection and contraction algorithms for quasivariational inequalities. *Appl. Set-Valued Anal. Optim.* **1** (2019), 63–76. doi:10.23952/asvao.1.2019.1.06.

[1] Department of Mathematics, School of Science
University of Phayao, Phayao, 56000, Thailand
Email address: damrongsak.ya@up.ac.th

[2] Department of Mathematics, School of Science
University of Phayao, Phayao, 56000, Thailand
Email address: tanakit.th@up.ac.th